UNIFIED FINITE ELEMENT DISCRETIZATIONS OF COUPLED DARCY-STOKES FLOW

TRYGVE KARPER, KENT–ANDRE MARDAL AND RAGNAR WINTHER

Abstract. In this paper we discuss some new finite element methods for flows which are governed by the linear stationary Stokes system on one part of the domain and by a second order elliptic equation derived from Darcy's law in the rest of the domain, and where the solutions in the two domains are coupled by proper interface conditions. All the methods proposed here utilize the same finite element spaces on the entire domain. In particular, we show how the coupled problem can be solved by using standard Stokes elements like the MINI element or the Taylor–Hood element in the entire domain. Furthermore, for all the methods the handling of the interface conditions are straightforward.

1. Introduction

The purpose of this paper is to discuss some new finite element discretizations of coupled Darcy–Stokes flow. The term "coupled Darcy–Stokes flow" refers to a flow which is governed by the Stokes equations in one part of the domain, while the flow is described by a standard second order elliptic equation, derived from Darcy's law and conservation of mass, on the rest of the domain. Furthermore, proper interface conditions have to be prescribed at the interface between the two regions.

Early numerical studies of the coupling of Darcy flow and Stokes flow can for example be found in [12, 22], while the more theoretical studies of such computations were initiated by the independent papers [15] and [16]. Actually, the approaches taken in these two papers are rather different. The method discussed in [16] is based on a standard finite element method for second order elliptic problems in the Darcy domain, and a standard mixed velocity–pressure formulation in the Stokes domain, while the methods discussed in [15] employ mixed finite element discretizations for both parts of the domain.

The development in [15] is based on a rigorous treatment of the weak saddle–point formulation of the corresponding continuous system. In particular, it is discussed how proper interface conditions lead to well posedness of the weak system. Since the stable families of finite elements for the Darcy problem and the Stokes problem usually are not the same, this approach easily leads to finite element discretizations with different choice of spaces for the two regions. In [15] such discretizations are proposed based on standard mixed elements for second order elliptic equations like the Raviart–Thomas

---

1991 *Mathematics Subject Classification.* 65N30, 76S05.

Key words and phrases. coupled Darcy–Stokes flow, alternative weak formulations, non–conforming finite elements.

Mardal has been supported by the Norwegian Research Council under the grant 170650.

spaces or the Brezzi–Douglas–Marini spaces for the Darcy region, and standard Stokes elements like the Taylor–Hood element or the MINI element for the Stokes region. A similar approach is basically taken in [13], but with the difference that the Bernardi–Raugel element is used for the Stokes region, while in [19, 20] variants of the discontinuous Galerkin method are proposed.

In [1] it is argued that finite element discretizations based on the same finite element spaces for both regions will have some advantages with respect to implementation. However, the difficulty with this approach is that most stable Stokes elements will not be stable in the Darcy region, and that most stable Darcy elements will not be convergent for the Stokes problem. In [1] it is suggested to use a C^0–element of Fortin [11], cf. also [2], to overcome this problem. This finite element space is defined with respect to a rectangular grid. On each rectangle the velocity belongs to a twelve dimensional space of reduced quadratics, while the pressure is approximated by piecewise constants. The properties of this method are carefully analyzed and studied by numerical experiments in [1]. A possible disadvantage of this discretization is that the method has to be properly modified near the interface between the two domains. In particular, the presence of vertex degrees of freedom leads to extra difficulties near the interface, cf. [1, Section 3]. The finite element discretizations proposed in this paper are similar to the method discussed in [1] in the sense that the same finite element spaces will be used throughout the entire domain Ω. We therefore refer to the discretizations as *unified finite element discretizations*. However, for the methods discussed here the treatment of the interface conditions is straightforward.

Throughout the paper we will consider the approximation of a flow in a region $\Omega \subset \mathbb{R}^2$, consisting of a porous region Ω_d, where the flow is a Darcy flow, and an open region $\Omega_s = \Omega \backslash \overline{\Omega}_d$, where the flow is governed by the linear stationary Stokes system. Hence, in Ω_d the Darcy velocity $\boldsymbol{u} = \boldsymbol{u}_d$ and the pressure $p = p_d$ satisfy

$$
\begin{aligned}
\mu \boldsymbol{K}^{-1}\boldsymbol{u}_d - \mathbf{grad}\, p_d &= \boldsymbol{f}, && \text{in} \quad \Omega_d,\\
\operatorname{div} \boldsymbol{u}_d &= g, && \text{in} \quad \Omega_d,\\
\boldsymbol{u}_d \cdot \boldsymbol{\nu} &= 0, && \text{on} \quad \partial\Omega \cap \partial\Omega_d,
\end{aligned}
\tag{1.1}
$$

where $\boldsymbol{\nu}$ is the outward unit normal vector on $\partial\Omega \cap \partial\Omega_d$, while in Ω_s the velocity/pressure $(\boldsymbol{u}, p) = (\boldsymbol{u}_s, p_s)$ is a solution of the system

$$
\begin{aligned}
-2\mu\ \operatorname{div}(\boldsymbol{\epsilon}(\boldsymbol{u}_s)) - \mathbf{grad}\, p_s &= \boldsymbol{f}, && \text{in} \quad \Omega_s,\\
\operatorname{div} \boldsymbol{u}_s &= g, && \text{in} \quad \Omega_s,\\
\boldsymbol{u}_s &= 0, && \text{on} \quad \partial\Omega \cap \partial\Omega_s, .
\end{aligned}
\tag{1.2}
$$

Here $\boldsymbol{\epsilon}(\boldsymbol{u}) = \frac{1}{2}\left(\mathbf{grad}\, \boldsymbol{u} + \mathbf{grad}\, \boldsymbol{u}^T\right)$ is the symmetric gradient operator, $\boldsymbol{K}$ is a uniformly positive definite permeability tensor, $\boldsymbol{f}$ is representing body forces, g represents sink or source terms, and $\mu > 0$ denotes the viscosity of the fluid.

The systems (1.1) and (1.2) are coupled at the interface between porous and open regions, i.e. at $\Gamma = \partial\Omega_s \cap \partial\Omega_d$. We will assume throughout the paper that Γ is a Lipschitz curve. The following interface conditions will be assumed:

$$\boldsymbol{u}_s \cdot \boldsymbol{\nu} = \boldsymbol{u}_d \cdot \boldsymbol{\nu} \quad \text{on } \Gamma, \tag{1.3}$$

$$2\mu \boldsymbol{\nu} \cdot \boldsymbol{\epsilon}(\boldsymbol{u}_s) \cdot \boldsymbol{\nu} = p_s - p_d \quad \text{on } \Gamma, \tag{1.4}$$

$$2\boldsymbol{\nu} \cdot \boldsymbol{\epsilon}(\boldsymbol{u}_s) \cdot \boldsymbol{\tau} = \alpha \boldsymbol{K}^{-\frac{1}{2}} \boldsymbol{u}_s \cdot \boldsymbol{\tau} \quad \text{on } \Gamma. \tag{1.5}$$

Here (1.3) represents mass conservation, (1.4) represents continuity of normal stress, and (1.5), with $\alpha > 0$, is the Beavers–Joseph–Saffmann condition [4, 21]. Moreover, $\boldsymbol{\tau}$ denotes the unit tangential vector at Γ and $\boldsymbol{\nu}$ the unit normal vector exterior to Ω_d.

The complete system given by (1.1)–(1.5) is the coupled Darcy–Stokes we will study below. In the weak formulation discussed in [15] the solution $\boldsymbol{u}_d \in \boldsymbol{H}(\mathrm{div})$, $\boldsymbol{u}_s \in \boldsymbol{H}^1$, and $p \in L^2$. Based on this formulation we will in Section 3 below introduce a new finite element discretization for the coupled system (1.1)–(1.5) by using the triangular non–conforming $\boldsymbol{H}^1$–space introduced in [17] for velocity and piecewise constants for pressure. Compared to the discretization proposed in [1], this method has the advantage that the velocity space, which is a conforming $\boldsymbol{H}(\mathrm{div})$–space, has no vertex degrees of freedom. As a consequence, there are no particular difficulties in modifying the method near the interface. The analysis given in this paper is restricted to two space dimension. However, a three dimensional analog of the non–conforming finite element space of [17] is discussed in [23].

Note that if the first equation of (1.1) holds then $\boldsymbol{u}_d$ can be eliminated and the second equation of (1.1) takes the form of a second order elliptic equation

$$\mathrm{div}\, \mu^{-1} \boldsymbol{K}\, \mathbf{grad}\, p_d = g', \quad \text{in} \quad \Omega_d, \tag{1.6}$$

where $g' = g - \mathrm{div}\, \mu^{-1} \boldsymbol{K} \boldsymbol{f}$. This is in fact the approach taken in [16], where the scalar equation (1.6) is approximated by a standard finite element method in the Darcy domain Ω_d, and a mixed finite element method for the Stokes equation is used in Ω_s. The second class of methods we will analyze below is closely related to this approach in the sense that the alternative weak formulation of the system (1.1)–(1.5) requires that the solution restricted to the Darcy domain, $(\boldsymbol{u}_d, p_d)$, is in $\boldsymbol{L}^2 \times H^1$, while $(u_s, p_s) \in \boldsymbol{H}^1 \times L^2$. However, in Section 4 we propose a discretization strategy where the variables $\boldsymbol{u}_d$ and p_d both are kept as unknowns in the discrete system, and where Darcy's law are only satisfied up to a given accuracy. In fact, by this approach we will propose a discretization of the full coupled system (1.1)–(1.5) where standard Stokes elements, like the MINI element or the Taylor–Hood element, can be used for the entire domain Ω. Finally, in Section 5 we present a some numerical examples.

2. Preliminaries

We will use $H^m = H^m(\Omega)$, with norm $\|\cdot\|_m$, to denote the Sobolev space of scalar functions on Ω with m derivatives belonging to the space $L^2(\Omega)$. The space $H_0^m = H_0^m(\Omega)$ denotes the closure of $C_0^\infty(\Omega)$ in H^m and is equipped with the semi–norm $|\cdot|_m$ derived from all derivatives of order m. Vector valued functions and spaces are written in boldface. By the notation L_0^2 we mean the functions in L^2 with mean value zero. We use $\langle \cdot, \cdot \rangle$ to denote the

L^2 inner product on scalar, vector and matrix valued functions as well as the duality pairing between H_0^m and its dual space. An extra subscript in inner products or norms, e.g., $\|\cdot\|_{m,T}$, means that the integration is performed over a domain T different from Ω. If T is Ω_s or Ω_d we simplify the notation further by only using the subscripts s or d, i.e., $\|\cdot\|_{m,d}$. For simplicity, the restrictions of a function v to the Darcy and Stokes regions, $v|_{\Omega_d}$ and $v|_{\Omega_s}$ are denoted by v_d and v_s, respectively.

If q is a scalar function, then $\mathbf{grad}\, q$ denotes the gradient of q, while $\operatorname{div} \boldsymbol{v} = \operatorname{trace} \mathbf{grad}\, \boldsymbol{v}$ denotes the divergence of the vector field $\boldsymbol{v}$. If we define the differential operators

$$\mathbf{curl}\, q = \begin{pmatrix} -\partial q/\partial x_2 \\ \partial q/\partial x_1 \end{pmatrix} \quad \text{and} \quad \operatorname{rot} \boldsymbol{v} = \frac{\partial \boldsymbol{v}_1}{\partial x_2} - \frac{\partial \boldsymbol{v}_2}{\partial x_1},$$

then, by Green's theorem

$$\int_\Omega \mathbf{curl}\, q \cdot \boldsymbol{v}\; dx = \int_\Omega q \operatorname{rot} \boldsymbol{v}\; dx - \int_{\partial\Omega} q(\boldsymbol{v} \cdot \boldsymbol{\tau})\; ds, \tag{2.1}$$

where s denote arc length. By direct calculation one may verify the identity

$$\operatorname{div} \boldsymbol{\epsilon} = \mathbf{grad} \operatorname{div} - \frac{1}{2} \mathbf{curl} \operatorname{rot}, \tag{2.2}$$

where the divergence of a matrix is defined as the divergence taken row–wise. Therefore,

$$\langle \boldsymbol{\epsilon}(\boldsymbol{u}), \boldsymbol{\epsilon}(\boldsymbol{v}) \rangle = \langle \operatorname{div} \boldsymbol{u}, \operatorname{div} \boldsymbol{v} \rangle + \frac{1}{2} \langle \operatorname{rot} \boldsymbol{u}, \operatorname{rot} \boldsymbol{v} \rangle, \quad \boldsymbol{u} \in \boldsymbol{H}_0^1, \boldsymbol{v} \in \boldsymbol{H}^1. \tag{2.3}$$

Below we will also use the spaces

$$\boldsymbol{H}(\operatorname{div}; \Omega) = \{\boldsymbol{v} \in \boldsymbol{L}^2(\Omega) : \operatorname{div} \boldsymbol{v} \in L^2(\Omega)\}$$

and

$$\boldsymbol{H}_0(\operatorname{div}; \Omega) = \{\boldsymbol{v} \in \boldsymbol{H}(\operatorname{div}; \Omega) : \boldsymbol{v} \cdot \boldsymbol{\nu} = 0 \text{ on } \partial\Omega\}.$$

We will next state the two weak formulations which we will use below to construct the new finite element methods for the coupled problem (1.1)–(1.5). The weak formulation which has the velocity $\boldsymbol{u}_d$ in $\boldsymbol{H}(\operatorname{div})$ is referred to as the $\boldsymbol{H}(\operatorname{div})$–formulation. This is exactly the formulation considered in [15]. More precisely, the velocity $\boldsymbol{u}$ will be required to belong to the space

$$\boldsymbol{V}^1 = \boldsymbol{V}^1(\Omega) = \{\boldsymbol{v} \in \boldsymbol{H}_0(\operatorname{div}; \Omega) : \boldsymbol{v}_s \in \boldsymbol{H}^1(\Omega_s), \boldsymbol{v} = 0 \text{ on } \partial\Omega_s \cap \partial\Omega\}.$$

Note that a piecewise smooth vector field $\boldsymbol{v} \in \boldsymbol{V}^1(\Omega)$ has to have a continuous normal component on the interface Γ. The corresponding norm is given by

$$\|\boldsymbol{v}\|_{\boldsymbol{V}^1}^2 = \|\boldsymbol{v}\|_0^2 + \|\operatorname{div} \boldsymbol{v}\|_0^2 + \|\mathbf{grad}\, \boldsymbol{v}\|_{0,s}^2.$$

Define a bilinear form $a : \boldsymbol{V}^1 \times \boldsymbol{V}^1 \to \mathbb{R}$ by

$$a(\boldsymbol{u}, \boldsymbol{v}) = \mu \langle \boldsymbol{K}^{-1} \boldsymbol{u}, \boldsymbol{v} \rangle_d + 2\mu \langle \boldsymbol{\epsilon}(\boldsymbol{u}), \boldsymbol{\epsilon}(\boldsymbol{v}) \rangle_s + \mu\alpha \langle \boldsymbol{K}^{-\frac{1}{2}} \boldsymbol{u}_s \cdot \boldsymbol{\tau}, \boldsymbol{v}_s \cdot \boldsymbol{\tau} \rangle_\Gamma.$$

The weak formulation of the coupled problem (1.1)–(1.5) discussed in [15] can be written:

Weak Formulation **2.1** ($\boldsymbol{H}(\mathrm{div})$–formulation)**.** *Find functions* $(\boldsymbol{u}, p) \in \boldsymbol{V}^1 \times L_0^2$ *such that, for all* $(\boldsymbol{v}, q) \in \boldsymbol{V}^1 \times L^2$

$$\begin{aligned} a(\boldsymbol{u}, \boldsymbol{v}) + \langle p, \operatorname{div} \boldsymbol{v} \rangle &= \langle \boldsymbol{f}, \boldsymbol{v} \rangle, \\ \langle q, \operatorname{div} \boldsymbol{u} \rangle &= \langle g, q \rangle. \end{aligned}$$

Note that in this formulation the boundary conditions on $\partial\Omega$ and the interface condition (1.3) are treated as essential conditions, while the interface conditions (1.4) and (1.5) are posed weakly. In Section 3 below we will propose a finite element method for the coupled problem (1.1)–(1.5) based on this formulation.

An alternative formulation of the coupled problem is posed using the velocity space

$$\boldsymbol{V}^2 = \boldsymbol{V}^2(\Omega) = \{\boldsymbol{v} \in \boldsymbol{L}^2(\Omega) : \boldsymbol{v}_s \in \boldsymbol{H}^1(\Omega_s), \boldsymbol{v} = 0 \text{ on } \partial\Omega_s \cap \partial\Omega\}, \tag{2.4}$$

with the corresponding norm

$$\|\boldsymbol{v}\|_{\boldsymbol{V}^2}^2 = \|\boldsymbol{v}\|_0^2 + \|\operatorname{\mathbf{grad}} \boldsymbol{v}\|_{0,s}^2.$$

The pressure space is

$$Q^2 = \{q \in L_0^2(\Omega) : q_d \in H^1(\Omega_d)\}, \tag{2.5}$$

with the norm

$$\|q\|_{Q^2}^2 = \|q\|_0^2 + \|\operatorname{\mathbf{grad}} q\|_{0,d}^2.$$

In this formulation the divergence constraint will be posed weakly in the form

$$\langle \operatorname{div} \boldsymbol{u}_s, q_s \rangle_s - \langle \boldsymbol{u}_d, \operatorname{\mathbf{grad}} q_d \rangle_d + \langle \boldsymbol{u}_s \cdot \boldsymbol{\nu}, q_d \rangle_\Gamma = \langle g, q \rangle$$

for all $q \in Q^2$. In fact, this relation also include a weak formulation of the interface condition (1.3), i.e. $\boldsymbol{u}_d \cdot \boldsymbol{\nu} = \boldsymbol{u}_s \cdot \boldsymbol{\nu}$ on Γ. We therefore obtain the following weak formulation of the system (1.1)–(1.5):

Weak Formulation **2.2** ($\boldsymbol{L}^2$–formulation)**.** *Find functions* $(\boldsymbol{u}, p) \in \boldsymbol{V}^2 \times Q^2$ *such that for all* $(\boldsymbol{v}, q) \in \boldsymbol{V}^2 \times Q^2$

$$\begin{aligned} a(\boldsymbol{u}, \boldsymbol{v}) + b(p, \boldsymbol{v}) &= \langle \boldsymbol{f}, \boldsymbol{v} \rangle, \\ b(q, \boldsymbol{u}) &= \langle g, q \rangle. \end{aligned}$$

Here the bilinear form a is exactly as above, and $b : Q^2 \times \boldsymbol{V}^2 \to \mathbb{R}$ is given by

$$b(p, \boldsymbol{v}) = \langle p_s, \operatorname{div} \boldsymbol{v}_s \rangle_s - \langle \operatorname{\mathbf{grad}} p_d, \boldsymbol{v}_d \rangle_d + \langle p_d, \boldsymbol{v}_s \cdot \boldsymbol{\nu} \rangle_\Gamma.$$

Note that in this alternative formulation all the three interface conditions (1.3)–(1.5) are expressed weakly. We will establish the existence and uniqueness of a weak solution by verifying the so–called Brezzi conditions [8]. From Korn's inequality, cf. [1] or [6], it follows that there is a positive constant C such that

$$\|\boldsymbol{v}_s\|_{1,s} \le C \left(\|\boldsymbol{\epsilon}(\boldsymbol{v}_s)\|_{0,s} + \|\boldsymbol{v}_s \cdot \boldsymbol{\tau}\|_{0,\Gamma} \right), \quad \boldsymbol{v} \in \boldsymbol{V}^2. \tag{2.6}$$

Hence, the coercivity of the bilinear form a,

$$a(\boldsymbol{v}, \boldsymbol{v}) \ge \alpha_2 \|\boldsymbol{v}\|_{\boldsymbol{V}^2}^2, \quad \boldsymbol{v} \in \boldsymbol{V}^2, \tag{2.7}$$

follows. Here α_2 is a positive constant. The second Brezzi condition that we need to verify is the inf–sup condition.

LEMMA **2.1.** *There is a constant $\beta_2 > 0$ such that for all $q \in Q^2$*

$$\sup_{\boldsymbol{v}\in \boldsymbol{V}^2} \frac{b(q,\boldsymbol{v})}{\|\boldsymbol{v}\|_{\boldsymbol{V}^2}} \geq \beta_2 \|q\|_{Q^2}, \quad \forall q \in Q^2. \tag{2.8}$$

Proof. Let $q \in Q^2$ be arbitrary. By the standard inf–sup condition for the Stokes problem, cf. [14, Chapter I.2.2], there is a $\boldsymbol{w} \in \boldsymbol{H}_0^1(\Omega) \subset \boldsymbol{V}^2$ such that

$$\operatorname{div} \boldsymbol{w} = q, \quad \text{in} \quad \Omega.$$

Furthermore, $\boldsymbol{w}$ satisfies a bound of the form

$$\|\boldsymbol{w}\|_{\boldsymbol{V}^2} \leq \|\boldsymbol{w}\|_1 \leq C_1 \|q\|_0. \tag{2.9}$$

Define $\boldsymbol{v} \in \boldsymbol{V}^2$ by $\boldsymbol{v}_s = \boldsymbol{w}_s$ and $\boldsymbol{v}_d = \boldsymbol{w}_d - \mathbf{grad}\, q_d$. It is now straightforward to check that

$$b(\boldsymbol{v}, q) = \|q\|_0^2 + \|\,\mathbf{grad}\, q_d\|_{0,d}^2 = \|q\|_Q^2.$$

Therefore the desired bound holds with $\beta_2 = 1/\max(1, C_1)$. □

The conditions (2.7) and (2.8), together with some obvious boundedness estimates on the bilinear forms a and b, implies that the ($\boldsymbol{L}^2$–formulation) above is well posed. Here it is assumed that the data $\boldsymbol{f}$ and g represents linear functionals on $\boldsymbol{V}^2$ and Q^2, respectively.

3. DISCRETIZATION IN THE $H(div)$ FORMULATION

In this section we will study finite element discretizations of the coupled Darcy–Stokes problem based on the $\boldsymbol{H}(\mathrm{div};\Omega)$ formulation. The finite element space $\boldsymbol{V}_h^1$, approximating $\boldsymbol{V}^1$, which we shall use will be the non–conforming $\boldsymbol{H}^1$–space used in [17] to approximate a family of singular perturbation problems of Stokes type, degenerating to a Darcy flow. The space $\boldsymbol{V}_h^1$ will be a subspace of $\boldsymbol{H}(\mathrm{div};\Omega)$, but the restrictions of functions in $\boldsymbol{V}_h^1$ to Ω_s will not be in $\boldsymbol{H}^1(\Omega_s)$. In this respect, the discretization is non–conforming.

In order to define the finite element spaces $\boldsymbol{V}_h^1$ let $\{\mathcal{T}_h\}$ be a shape regular family of triangulations of Ω, where the mesh parameter h represents the maximal diameter of triangles $T \in \mathcal{T}_h$. We will assume throughout the paper that each triangulation $\mathcal{T}_h$ has the property that the interface Γ is composed of mesh edges, such that the interior of each triangle is either in Ω_d or Ω_s. We let $\mathcal{T}_h^d$ and $\mathcal{T}_h^s$ be the corresponding induced triangulations of Ω_d and Ω_s, respectively, while Γ_h denote the set of edges on Γ.

On each triangle $T \in \mathcal{T}_h$ the restriction of functions in $\boldsymbol{V}_h^1$ belongs to the polynomial space

$$\boldsymbol{V}^1(T) = \{\boldsymbol{v} \in \mathbb{P}_3^2 : \operatorname{div} \boldsymbol{v} \in \mathbb{P}_0, (\boldsymbol{v}\cdot\boldsymbol{\nu})|_e \in \mathbb{P}^1, \forall e \in \mathcal{E}(T)\}, \tag{3.1}$$

where $\mathcal{E}(T)$ denotes the set of edges of T. The space $\boldsymbol{V}^1(T)$ has dimension nine and each element $\boldsymbol{v}$ is determined by the following degrees of freedom:

- $\int_e (\boldsymbol{v}\cdot\boldsymbol{\nu}) t^k \, ds, \quad k = 0, 1$ and for all $e \in \mathcal{E}(T)$,
- $\int_e \boldsymbol{v}\cdot\boldsymbol{\tau} \, ds$ for all $e \in \mathcal{E}(T)$,

cf. Figure 3.1 on the facing page. Here $\boldsymbol{\nu}$ and $\boldsymbol{\tau}$ are unit normal and tangent vectors on the edges.

The finite element space $\boldsymbol{V}_h^1$, associated with the triangulation $\mathcal{T}_h$, is the set of all piecewise polynomial vector fields $\boldsymbol{v}$ such that

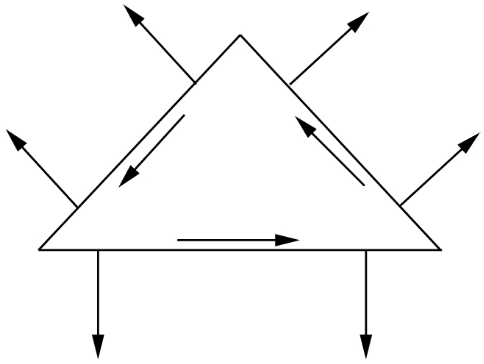

FIGURE 3.1. Degrees of freedom for $\boldsymbol{V}^1(T)$

- $\boldsymbol{v}|_T \in \boldsymbol{V}(T), \quad \forall T \in \mathcal{T}_h,$
- $\int_e (\boldsymbol{v}\cdot\boldsymbol{\nu}) t^k \, ds$ is continuous for $k = 0, 1$ and for all $e \in \mathcal{E}(\mathcal{T}_h)$,
- $\int_e \boldsymbol{v}\cdot\boldsymbol{\tau} \, ds$ is continuous for all $e \in \mathcal{E}(\mathcal{T}_h) \setminus \Gamma_h$,

where $\mathcal{E}(\mathcal{T}_h)$ is the set of edges in $\mathcal{T}_h$. Hence, the elements of $\boldsymbol{V}_h^1$ has continuous normal component over each edge, weakly continuous tangential components in the interior of each region, and completely discontinuous tangential component over the interface Γ.

Let also $Q_h^1 \subset L_0^2$ denote the space of piecewise constants with respect to the triangulation $\mathcal{T}_h$. We then obtain the following finite element method:

FINITE ELEMENT FORMULATION **3.1.** *Find functions $(\boldsymbol{u}_h, p_h) \in \boldsymbol{V}_h^1 \times Q_h^1$ such that for all $(\boldsymbol{v}, q) \in \boldsymbol{V}_h^1 \times Q_h^1$*

$$\begin{aligned} a(\boldsymbol{u}_h, \boldsymbol{v}) + \langle p_h, \operatorname{div} \boldsymbol{v}\rangle &= \langle \boldsymbol{f}, \boldsymbol{v}\rangle, \\ \langle q, \operatorname{div} \boldsymbol{u}_h\rangle &= \langle g, q\rangle. \end{aligned}$$

Here a is the bilinear form introduced above, except that the term with symmetric gradients has to be computed element–wise, i.e.

$$\begin{aligned} a(\boldsymbol{u}, \boldsymbol{v}) =& \mu\langle \boldsymbol{K}^{-1}\boldsymbol{u}, \boldsymbol{v}\rangle_d + \mu\alpha\langle \boldsymbol{K}^{-\frac{1}{2}}\boldsymbol{u}_s\cdot\boldsymbol{\tau}, \boldsymbol{v}_s\cdot\boldsymbol{\tau}\rangle_\Gamma \\ &+ \sum_{T\in\mathcal{T}_h^s} 2\mu\langle \boldsymbol{\epsilon}(\boldsymbol{u}), \boldsymbol{\epsilon}(\boldsymbol{v})\rangle_T. \end{aligned}$$

The discretization is stable in the sense of [8] if there exists constants $\alpha_1, \beta_1 > 0$, independent of h, such that:

$$a(\boldsymbol{v}, \boldsymbol{v}) \geq \alpha_1 \|\boldsymbol{v}\|_{\boldsymbol{V}_h^1}^2, \quad \boldsymbol{v} \in \boldsymbol{Z}_h^1, \tag{3.2}$$

and

$$\sup_{\boldsymbol{v}\in\boldsymbol{V}_h^1} \frac{\langle q, \operatorname{div}\rangle \boldsymbol{v}}{\|\boldsymbol{v}\|_{\boldsymbol{V}_h^1}} \geq \beta_1 \|q\|_0, \quad q \in Q_h^1, \tag{3.3}$$

where $Z_h^1 = \{\boldsymbol{z} \in \boldsymbol{V}_h^1 : \langle q, \operatorname{div} \boldsymbol{z}\rangle = 0, \quad \forall q \in Q_h^1\}$ is the space of weakly divergence free elements of $\boldsymbol{V}_h^1$. Here the norm $\|\cdot\|_{\boldsymbol{V}_h^1}$ is the broken norm corresponding to $\|\cdot\|_{\boldsymbol{V}^1}$, i.e.

$$\|\boldsymbol{v}\|_{\boldsymbol{V}_h^1}^2 = \|\boldsymbol{v}\|_0^2 + \|\operatorname{div} \boldsymbol{v}\|_0^2 + \sum_{T\in\mathcal{T}_h^s} \|\mathbf{grad}\, \boldsymbol{v}\|_{0,T}^2.$$

By construction, $\operatorname{div} \boldsymbol{V}_h^1 \subset Q_h^1$. Furthermore, the space $\boldsymbol{V}_h^1$ admits a discrete Poincaré inequality of the form

$$\|\boldsymbol{v}\|_{0,s}^2 \le c \left(\sum_{T \in \mathcal{T}_h^s} \|\,\mathbf{grad}\,\boldsymbol{v}\|_{0,T}^2 + \|\boldsymbol{v}_s \cdot \boldsymbol{\tau}\|_{0,\Gamma}^2 \right),$$

where the constant c is independent of h, cf. [7, Theorem 5.1]. Therefore, the condition (3.2) will follow from a Korn's inequality of the form

$$\sum_{T \in \mathcal{T}_h^s} \|\,\mathbf{grad}\,\boldsymbol{v}\|_{0,T}^2 \le C \left(\sum_{T \in \mathcal{T}_h^s} \|\boldsymbol{\epsilon}(\boldsymbol{v})\|_{0,T}^2 + \|\boldsymbol{v}_s \cdot \boldsymbol{\tau}\|_{0,\Gamma}^2 \right), \quad \boldsymbol{v} \in \boldsymbol{V}_h^1. \tag{3.4}$$

Basically, Korn's inequality for the non–conforming $\boldsymbol{H}^1$ space $\boldsymbol{V}_h^1$ was established in [18] as an application of the general results of [6]. However, the Korn inequality established in [18] was of the form

$$\sum_{T \in \mathcal{T}_h^s} \|\,\mathbf{grad}\,\boldsymbol{u}_s\|_{0,T}^2 \le C \left(\sum_{T \in \mathcal{T}_h^s} \|\boldsymbol{\epsilon}(\boldsymbol{u}_s)\|_{0,T}^2 + \|\boldsymbol{u}_s\|_{0,s}^2) \right).$$

Here we need Korn's inequality in the slightly different form (3.4), where we only have boundary control of the functions in the kernel of the symmetric gradient $\boldsymbol{\epsilon}$, i.e. of rigid motions.

LEMMA **3.1.** *There exists a positive constant C, independent of h, such that the bound* (3.4) *holds.*

Proof. We first note that the desired bound (3.4) will follow from an inequality of the form

$$\sum_{T \in \mathcal{T}_h^s} \|\,\mathbf{grad}\,\boldsymbol{v}\|_{0,T}^2 \le C_1 \left(\sum_{T \in \mathcal{T}_h^s} \|\boldsymbol{\epsilon}(\boldsymbol{v})\|_{0,T}^2 + |\int_{\Omega_s} \operatorname{rot} \boldsymbol{v}\; dx|^2 \right) \tag{3.5}$$

for all $\boldsymbol{v} \in \boldsymbol{V}_h^1$, and by applying (2.1) with $q \equiv 1$.

The bound (3.5) is indeed established in [6, Theorem 3.1], but only for non–conforming $\boldsymbol{H}^1$ spaces where all functions are weakly continuous with respect to linear functions on the mesh edges. The space $\boldsymbol{V}_h^1$ we discuss here does not have this property, since the tangential component is only weakly continuous with respect to constants. However, the basic observation done in [18] was that this weak continuity condition can be relaxed throughout the discussion given in [6] such that the present element applies. Therefore, all the Korn inequalities derived in [6], in particular (3.5), holds for the finite element space $\boldsymbol{V}_h^1$. □

As observed above (3.4) implies (3.2). The other stability condition, (3.3), will follow from the construction of a suitable interpolation operator $\Pi_h : \boldsymbol{H}^1(\operatorname{div};\Omega) \to \boldsymbol{V}_h^1$ which satisfies the relation

$$\langle \operatorname{div} \Pi_h \boldsymbol{v}, q \rangle = \langle \operatorname{div} \boldsymbol{v}, q \rangle, \quad \boldsymbol{v} \in \boldsymbol{H}^1(\operatorname{div};\Omega),\ q \in Q_h^1. \tag{3.6}$$

Here $\boldsymbol{H}^1(\operatorname{div};\Omega) = \{\boldsymbol{v} \in \boldsymbol{H}(\operatorname{div};\Omega) : v_d \in \boldsymbol{H}^1(\Omega_d),\ v_s \in \boldsymbol{H}^1(\Omega_s)\ \}$. The operator Π_h is defined from the degrees of freedom of the space $\boldsymbol{V}_h^1$, i.e.

- $\int_e (\Pi_h \boldsymbol{v} \cdot \boldsymbol{\nu}) t^k\, ds = \int_e (\boldsymbol{v} \cdot \boldsymbol{\nu}) t^k\, ds, \quad k = 0, 1 \quad e \in \mathcal{E}(\mathcal{T}_h),$

- $\int_e (\Pi_h \boldsymbol{v} \cdot \boldsymbol{\tau})\, ds = \int_e (\boldsymbol{v} \cdot \boldsymbol{\tau})\, ds, \quad e \in \mathcal{E}(\mathcal{T}_h)$,

with the obvious modification that two one sided values are used for the tangential component if $e \in \Gamma_h$. This operator is uniformly bounded as an operator from $\boldsymbol{H}^1(\mathrm{div}; \Omega)$ to $\boldsymbol{V}_h^1$. In fact, it follows from the analysis of the corresponding operator in [17] that

$$\|\boldsymbol{v} - \Pi_h \boldsymbol{v}\|_{j,T} \le ch^{k-j} |\boldsymbol{v}|_{k,T}, \quad 0 \le j \le 1 \le k \le 2, T \in \mathcal{T}_h, \tag{3.7}$$

where the constant c is independent of $\boldsymbol{v}$, h, and T.

THEOREM **3.1.** *The family of finite element spaces* $\{\boldsymbol{V}_h^1 \times Q_h^1\}$ *satisfies the stability conditions* (3.2) *and* (3.3).

Proof. We have already established (3.2). Furthermore, for each $q \in Q_h^1$ there is a $\boldsymbol{v} \in \boldsymbol{H}^1(\Omega) \subset \boldsymbol{H}^1(\mathrm{div}; \Omega)$ such that $\mathrm{div}\, \boldsymbol{v} = q$ and $\|\boldsymbol{v}\|_1 \le c\|q\|_0$, cf. [14, Chapter I.2.2]. Then, $\Pi_h \boldsymbol{v} \in \boldsymbol{V}_h^1$, $\mathrm{div}\, \Pi_h \boldsymbol{v} = q$, and $\|\Pi_h \boldsymbol{v}\|_0 \le c\|q\|_0$, and this implies condition (3.3). □

Let $(\boldsymbol{u}, p) \in \boldsymbol{V}^1 \times L_0^2$ be a weak solution of the coupled system (1.1)–(1.5). For any $\boldsymbol{v} \in \boldsymbol{V}_h^1$ define the consistency error $E_h(\boldsymbol{v}) = E_h(\boldsymbol{u}, p; \boldsymbol{v})$ by

$$E_h(\boldsymbol{v}) \equiv a(\boldsymbol{u}, \boldsymbol{v}) + \langle p, \mathrm{div}\, \boldsymbol{v} \rangle - \langle \boldsymbol{f}, \boldsymbol{v} \rangle.$$

For the rest of the discussion of this section we assume that $\boldsymbol{u}_s \in \boldsymbol{H}^2(\Omega_s)$ and $p \in H^1(\Omega)$. Then, from an integration by parts argument we derive that $E_h(\boldsymbol{v})$ is alternatively given as

$$E_h(\boldsymbol{v}) \equiv \mu \sum_{e \in \mathcal{E}(\mathcal{T}_h^s)} \int_e (\mathrm{rot}\, \boldsymbol{u}_s)[\boldsymbol{v} \cdot \boldsymbol{\tau}]_e\, ds,$$

where $[\boldsymbol{v} \cdot \boldsymbol{\tau}]_e$ denotes the jump of $\boldsymbol{v} \cdot \boldsymbol{\tau}$ if e is an edge in the interior of Ω_s, while it denotes $\boldsymbol{v}_s \cdot \boldsymbol{\tau}$ if $e \in \Gamma_h$. Furthermore, from [17, Lemma 5.1] it follows that

$$\sup_{\boldsymbol{v} \in \boldsymbol{V}_h^1} \frac{|E_h(\boldsymbol{v})|}{\|\boldsymbol{v}\|_a} \le ch \|\mathrm{rot}\, \boldsymbol{u}\|_{1,s}, \tag{3.8}$$

where the constant c is independent of h. Here $\|\boldsymbol{v}\|_a^2 = a(\boldsymbol{v}, \boldsymbol{v})$.

Let $(\boldsymbol{u}_h, p_h) \in \boldsymbol{V}_h^1 \times Q_h^1$ be the corresponding solution. Then

$$\mathrm{div}\, \boldsymbol{u}_h = P_h\, \mathrm{div}\, \boldsymbol{u} = \mathrm{div}\, \Pi_h \boldsymbol{u},$$

where P_h is the L^2–projection onto Q_h^1. As a consequence,

$$\|\mathrm{div}(\boldsymbol{u} - \boldsymbol{u}_h)\|_0 \le ch \|\mathrm{div}\, \boldsymbol{u}\|_1, \tag{3.9}$$

where the constant c is independent of h.

For any $\boldsymbol{v} \in \boldsymbol{V}_h^1$ we have that

$$a(\boldsymbol{u} - \boldsymbol{u}_h, \boldsymbol{v}) + \langle p - p_h, \mathrm{div}\, \boldsymbol{v} \rangle = E_h(\boldsymbol{v}). \tag{3.10}$$

By utilizing the fact that $\mathrm{div}(\Pi_h \boldsymbol{u} - \boldsymbol{u}_h) = 0$ we obtain that

$$a(\boldsymbol{u} - \boldsymbol{u}_h, \Pi_h \boldsymbol{u} - \boldsymbol{u}_h) = E_h(\Pi_h \boldsymbol{u} - \boldsymbol{u}_h),$$

and hence we obtain from Cauchy–Schwarz inequality that

$$\|\Pi_h \boldsymbol{u} - \boldsymbol{u}_h\|_a \le \|\boldsymbol{u} - \Pi_h \boldsymbol{u}\|_a + \sup_{\boldsymbol{v} \in \boldsymbol{V}_h^1} \frac{|E_h(\boldsymbol{v})|}{\|\boldsymbol{v}\|_a}. \tag{3.11}$$

From this error bound we easily obtain the following error estimates.

THEOREM **3.2.** *There is a constant c, independent of h, such that*

$$\|\boldsymbol{u}-\boldsymbol{u}_h\|_0 + \sum_{T\in T_h^s} \|\mathbf{grad}(\boldsymbol{u}-\boldsymbol{u}_h)\|_{0,T} \le ch\left(\|\boldsymbol{u}\|_{1,d} + \|\boldsymbol{u}\|_{2,s}\right), \tag{3.12}$$

and

$$\|p-p_h\|_0 \le ch\left(\|p\|_1 + \|\boldsymbol{u}\|_{1,d} + \|\boldsymbol{u}\|_{2,s}\right). \tag{3.13}$$

Proof. From (3.7), (3.9), and a standard trace inequality we obtain

$$\begin{aligned} \|\Pi_h\boldsymbol{u}-\boldsymbol{u}\|_a, \|\Pi_h\boldsymbol{u}-\boldsymbol{u}\|_{\boldsymbol{V}_h^1} &\le ch(\|\boldsymbol{u}\|_{1,d} + \|\boldsymbol{u}\|_{2,s} + \|\boldsymbol{u}_s\|_{1,\Gamma}) \\ &\le ch(\|\boldsymbol{u}\|_{1,d} + \|\boldsymbol{u}\|_{2,s}). \end{aligned} \tag{3.14}$$

By combining this with (3.8) and (3.11) we obtain that

$$\|\Pi_h\boldsymbol{u}-\boldsymbol{u}_h\|_a \le ch(\|\boldsymbol{u}\|_{1,d} + \|\boldsymbol{u}\|_{2,s}), \tag{3.15}$$

while the stability condition (3.2) implies that

$$\|\Pi_h\boldsymbol{u}-\boldsymbol{u}_h\|_{\boldsymbol{V}_h^1} \le \alpha_1^{-1/2}\|\Pi_h\boldsymbol{u}-\boldsymbol{u}_h\|_a. \tag{3.16}$$

Hence, it follows by (3.14), (3.15), (3.16) and the triangle inequality that

$$\|\boldsymbol{u}-\boldsymbol{u}_h\|_{\boldsymbol{V}_h^1} \le \|\Pi_h\boldsymbol{u}-\boldsymbol{u}\|_{\boldsymbol{V}_h^1} + \|\Pi_h\boldsymbol{u}-\boldsymbol{u}_h\|_{\boldsymbol{V}_h^1} \le ch\left(\|\boldsymbol{u}\|_{1,d} + \|\boldsymbol{u}\|_{2,s}\right),$$

and this implies (3.12).

The error estimate (3.13) follows by standard arguments, where we use the stability condition (3.3), (3.10), and (3.12) to estimate $\|P_hp-p_h\|_0$. □

4. DISCRETIZATION IN THE L^2 FORMULATION

We now consider a discretization based on the alternative formulation referred to as the L^2 formulation above. In this case we will only consider conforming discretizations, i.e. the finite element spaces will satisfy $\boldsymbol{V}_h^2 \subset \boldsymbol{V}^2$ and $Q_h^2 \subset Q^2$.

FINITE ELEMENT FORMULATION **4.1.** *Find functions $(\boldsymbol{u}_h, p_h) \in \boldsymbol{V}_h^2 \times Q_h^2$ such that for all $(\boldsymbol{v}, q) \in \boldsymbol{V}_h^2 \times Q_h^2$*

$$\begin{aligned} a(\boldsymbol{u}_h, \boldsymbol{v}) + b(\boldsymbol{v}, p_h) &= \langle \boldsymbol{f}, \boldsymbol{v}\rangle, \\ b(\boldsymbol{u}_h, q) &= \langle g, q\rangle. \end{aligned}$$

If $\boldsymbol{V}_h^2 \subset \boldsymbol{V}^2$ then the bound (2.7) will hold for all $\boldsymbol{v} \in \boldsymbol{V}_h^2$. Therefore, in this case the discretization will be stable if the second Brezzi condition holds, i.e. we need to establish that there exists a positive constant $\beta_2' > 0$ such that

$$\sup_{\boldsymbol{v}\in\boldsymbol{V}_h^2} \frac{b(q,\boldsymbol{v})}{\|\boldsymbol{v}\|_{\boldsymbol{V}^2}} \ge \beta_2'\|q\|_{Q^2}, \quad \forall q \in Q_h^2. \tag{4.1}$$

We observe that common Stokes elements such as the MINI element or the Taylor–Hood element will indeed produce conforming discretizations of the coupled Darcy–Stokes problem in this formulation. Below we will discuss the convergence properties of the discretization derived from the MINI element. In a similar manner, it is also possible to derive convergence estimates for the Taylor–Hood element.

For the MINI element, introduced in [3], the velocity space consists of all functions of the form

$$\boldsymbol{v} = \boldsymbol{v}^0 + \sum_{T \in \mathcal{T}_h} \boldsymbol{c}_T b_T, \tag{4.2}$$

where $\boldsymbol{v}^0$ is a continuous piecewise linear vector field with respect to $\mathcal{T}_h$, b_T is the cubic bubble function on the triangle T, and $\boldsymbol{c}_T$ is a constant vector. In the present setting we will modify this space by relaxing the continuity over the interface such that all functions in $\boldsymbol{V}_h^2$ are allowed to be discontinuous across Γ. The corresponding pressure space Q_h^2 consists of continuous piecewise linear functions on Ω_d and Ω_s, but with no continuity requirement across Γ. Notice that we still have that $\boldsymbol{V}_h^2 \subset \boldsymbol{V}^2$ and $Q_h^2 \subset Q_h$.

The space $\boldsymbol{V}_h^2$ can be expressed as a direct sum, $\boldsymbol{V}_h^2 = \boldsymbol{V}_h^0 \oplus \boldsymbol{V}_h^b$, where $\boldsymbol{V}_h^0$ is the space of piecewise linear vector fields which are continuous on Ω_d and Ω_s, and where $\boldsymbol{V}_h^b$ denotes the span of the cubic bubble functions. Let $P_h^b : \boldsymbol{L}^2 \to \boldsymbol{V}_h^b$ be defined by

$$\int_T P_h^b \boldsymbol{v}\, dx = \int_T \boldsymbol{v}\, dx, \quad \forall T \in \mathcal{T}_h. \tag{4.3}$$

This operator is uniformly bounded in $\mathcal{L}(\boldsymbol{L}^2(\Omega), \boldsymbol{L}^2(\Omega))$ with respect to the mesh parameter h. The stability properties of the MINI element can be derived from a projection operator $\Pi_h : \boldsymbol{L}^2(\Omega) \to \boldsymbol{V}_h^2$ of the form

$$\Pi_h \boldsymbol{v} = I_h \boldsymbol{v} + P_h^b(\boldsymbol{v} - I_h \boldsymbol{v}),$$

where I_h is the Cléments interpolant mapping $\boldsymbol{L}^2(\Omega)$ onto $\boldsymbol{V}_h^0$. The operator I_h is uniformly bounded on both L^2 and H^1. In fact, it satisfies an estimate of the form

$$\|I_h \boldsymbol{v} - \boldsymbol{v}\|_{j,T} \le c h_T^{m-j} \|\boldsymbol{v}\|_{m,T^*}, \quad 0 \le j \le m \le 1, \qquad T \in \mathcal{T}_h, \tag{4.4}$$

cf [5, 10], where the constant c is independent of h. Here h_T is the diameter of the triangle T, while T^* is the domain of the macro–element consisting of all the triangles intersecting T, i.e.

$$T^* = \cup\{T' : T' \in \mathcal{T}_h,\, T' \cap T \ne \emptyset\ \}.$$

It is a consequence of the shape regularity of the family $\{\mathcal{T}_h\}$ that the decomposition $\{T^*\}_{T \in \mathcal{T}_h}$ of $\bar{\Omega}$, has a uniform overlap property, i.e. there is a $N > 0$, independent of h, such that no $x \in \bar{\Omega}$ belongs to more N of the sets T^*. It follows from the properties of the operators P_h^b and I_h that Π_h is uniformly bounded in L^2. In fact, for all $T \in \mathcal{T}_h$ we have from (4.4) that

$$\begin{aligned} \|\Pi_h \boldsymbol{v}\|_{1,T} &\le \|I_h \boldsymbol{v}\|_{1,T} + \|P_h^b(\boldsymbol{v} - I_h \boldsymbol{v})\|_{1,T} \\ &\le c\left(\|\boldsymbol{v}\|_{1,T^*} + h_T^{-1} \|P_h^b(\boldsymbol{v} - I_h \boldsymbol{v})\|_{0,T}\right) \\ &\le c\|\boldsymbol{v}\|_{1,T^*}, \end{aligned}$$

and hence it follows from the uniform overlap property of the decomposition $\{T^*\}$ that Π_h is also uniformly bounded in H^1.

In the present setting we need to modify the operator Π_h near the interface Γ. Recall that there is no continuity requirement over the interface Γ for functions in $\boldsymbol{V}_h^2$. Therefore, we can define define two independent operators

Π_h^d and Π_h^s, of the form above with respect to the domains Ω_d and Ω_s, respectively, and then let Π_h be given by

$$\Pi_h \boldsymbol{v} = \Pi_h^d \boldsymbol{v}_d + \Pi_h^s \boldsymbol{v}_s.$$

From the discussion above it then follows that the operator $\Pi_h : \boldsymbol{V}^2 \to \boldsymbol{V}_h^2$ is uniformly bounded, i.e. there is a constant c such that

$$\|\Pi_h \boldsymbol{v}\|_{\boldsymbol{V}^2} \le c\|\boldsymbol{v}\|_{\boldsymbol{V}^2}. \tag{4.5}$$

THEOREM **4.1.** *The family of elements $\{\boldsymbol{V}_h^2 \times Q_h^2\}$ satisfy the stability condition* (4.1)*.*

Proof. It is straightforward to check that for any $\boldsymbol{v} \in \boldsymbol{V}^2$ and $q \in Q_h^2$ we have

$$b(q, \Pi_h v) = -\langle \Pi_h \boldsymbol{v}, \mathbf{grad}\, q_d\rangle_d - \langle \Pi_h \boldsymbol{v}, \mathbf{grad}\, q_s\rangle_s = b(q, v).$$

Therefore the stability condition (4.1) follows from Lemma 2.1 and (4.5). □

From the stability conditions (2.7) and (4.1) it follows that the discrete solution $(\boldsymbol{u}_h, p_h) \in \boldsymbol{V}_h^2 \times Q_h^2$ satisfies a quasi optimal estimate of the form

$$\|\boldsymbol{u} - \boldsymbol{u}_h\|_{\boldsymbol{V^2}} + \|p - p_h\|_{Q^2} \le C \inf_{(\boldsymbol{v},q)\in \boldsymbol{V}_h^2\times Q_h^2} \left(\|\boldsymbol{u} - \boldsymbol{v}\|_{\boldsymbol{V^2}} + \|p - q\|_{Q^2}\right).$$

Here $(\boldsymbol{u}, p) \in \boldsymbol{V}^2 \times Q^2$ is the corresponding continuous solution, and the mesh independent constant C depends on the stability constants α_2 and β_2', cf. [8, 9]. In particular, if $(\boldsymbol{u}_s, p_s) \in \boldsymbol{H}^2(\Omega_s) \times H^1(\Omega_s)$, and $(\boldsymbol{u}_d, p_d) \in \boldsymbol{H}^1(\Omega_d) \times H^2(\Omega_d)$ we obtain a linear convergence estimate of the form

$$\|\boldsymbol{u} - \boldsymbol{u}_h\|_{\boldsymbol{V^2}} + \|p - p_h\|_{Q^2} \le ch\left(\|\boldsymbol{u}_d\|_{1,d} + \|\boldsymbol{u}_s\|_{2,s} + \|p_d\|_{2,d} + \|p_s\|_{1,s}\right).$$

5. Numerical experiments

We end the paper by a few numerical experiments. For simplicity we choose $\Omega = [0, 1] \times [0, 1]$, $\mu = \alpha = 1$, and the permeability tensor $\boldsymbol{K}$ is taken to be the identity. Furthermore, in all the examples we use a uniform grid. In order to make it simpler to generate analytic solutions we generalize the conditions (1.4)–(1.5) to allow for more general interface conditions of the form

$$2\mu\boldsymbol{\nu} \cdot \boldsymbol{\epsilon}(\boldsymbol{u}_s) \cdot \boldsymbol{\nu} = p_s - p_d + g_1 \quad \text{on } \Gamma,$$
$$2\boldsymbol{\nu} \cdot \boldsymbol{\epsilon}(\boldsymbol{u}_s) \cdot \boldsymbol{\tau} = \alpha \boldsymbol{K}^{-\frac{1}{2}} \boldsymbol{u}_s \cdot \boldsymbol{\tau} + g_2 \quad \text{on } \Gamma,$$

where g_1 and g_2 are given functions on Γ.

In the following we mostly report estimated convergence rates in different norms rather than the full error at each grid level. These rates are estimated by a simple least–squares fit of the form ch^{rate} to the norms of the errors as functions of h, where h ranges from 1/4 to 1/32. We first consider a couple of examples where the interface Γ is a straight line. These examples were also studied in [1]. For these examples the domain is divided into two regions by the line $x = 0.5$, with Ω_s to the right and Ω_d to the left. For Test Case 1 we choose $p = e^x \sin(x + y)$, $\boldsymbol{u}_s = (\cos(xy), e^{x+y})^t$, and $\boldsymbol{u}_d = (\cos(xy), 0)^t$, while for Test Case 2 we have $p = \cos(x^2 y)$, $\boldsymbol{u}_s = (\sin(x^2 y), \cos(x^2 y))^t$, and $\boldsymbol{u}_d = (\sin(x^2 y), e^{x+y})^t$. Note that both these solutions satisfy the interface condition (1.3). The estimated convergence rates are given in Table 1. Note

Case	$\|E_p\|_0$	$\|E_{\boldsymbol{u}}\|_0$	$\|\operatorname{div} E_{\boldsymbol{u}}\|_0$	$\|\mathbf{grad}\, E_{\boldsymbol{u}}\|_0$
1	1.0	2.0	1.0	1.0
2	1.1	2.0	1.0	1.1

TABLE 1. The estimated convergence rates in Test-Cases 1-2. Here and below E denotes the error in the subscript variable.

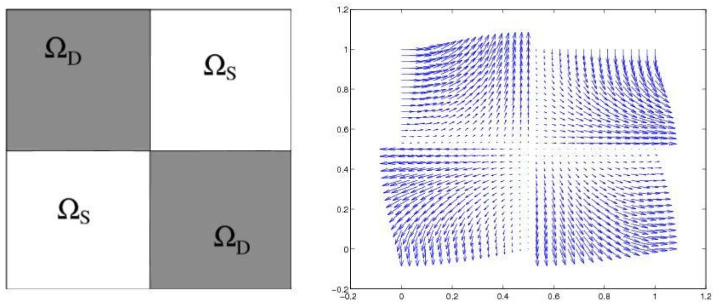

FIGURE 5.1. To the left is the domain configuration in Test-Case 3. The figure on the right is the obtained velocity solution for this case.

Case	p_s	p_d	$\boldsymbol{u}_s$	$\boldsymbol{u}_d$
3	1	0	$\begin{pmatrix}(x-\frac{1}{2})\sin(\pi y)\\(y-\frac{1}{2})\cos(\pi x)\end{pmatrix}$	$\begin{pmatrix}(x-\frac{1}{2})\cos(\pi y)\\(y-\frac{1}{2})\sin(\pi x)\end{pmatrix}$

TABLE 2. The analytical solution in Test-Case 3.

that the estimates (3.9)–(3.13) all predicts linear convergence. However, this example indicates that the L^2 error in velocity is actually second order accurate.

Next, we consider an example where the interface Γ is more complex. In this case the domain configuration has a checkerboard pattern, cf. Figure 5.1. The exact solution, satisfying the interface condition (1.3), is given in Table 2. The obtained errors and estimated convergence rates are given in Table 3, and, compared to what we observed above, the convergence properties do not seem to be essentially effected by the increased complexity of Γ.

Finally, we test the alternative discretization discussed in Section 4 using the MINI element. The estimated convergence rates for the Test–Cases 1–3 are given in Table 4. As expected we obtain linear convergence in the appropriate norms. However, note that in this case we do not seem to obtain convergence of the global L^2 norm of $\operatorname{div}(\boldsymbol{u}-\boldsymbol{u}_h)$. This is consistent with the convergence results of Section 4.

h	$\|E_p\|_0$	$\|E_{\boldsymbol{u}}\|_0$	$\|\operatorname{div} E_{\boldsymbol{u}}\|_0$	$\|\mathbf{grad}\, E_{\boldsymbol{u}}\|_0$
1/4	6.6e-1	6.7e-2	1.8e-1	3.1e-1
1/8	2.0e-1	1.8e-2	9.0e-2	1.5e-1
1/16	6.8e-2	4.5e-3	4.5e-2	7.3e-2
1/32	2.8e-2	1.1e-3	2.2e-2	3.6e-2
Rate:	1.7	2.0	1.0	1.0

TABLE 3. The obtained errors and estimated convergence rates in Test-Case 3.

Case	$\|E_p\|_0$	$\|E_p\|_{Q^2}$	$\|E_{\boldsymbol{u}}\|_0$	$\|\operatorname{div} E_{\boldsymbol{u}}\|_0$	$\|E_{\boldsymbol{u}}\|_{\boldsymbol{V}^2}$
1	1.6	1.0	1.0	0.025	1.0
2	1.8	1.1	1.0	0.011	1.0
3	1.8	1.6	1.1	0.044	1.0

TABLE 4. The convergence rates obtained by the MINI discretization in Test-Cases 1-3.

References

[1] T. Arbogast and D. S. Brunson. A computational method for approximating a Darcy-Stokes system governing a vuggy porous medium. *ICES Report 03–47, University of Texas, Austin*, 2003.

[2] T. Arbogast and M. Wheeler. A family of rectangular mixed elements with a continuous flux for second order elliptic problems. *SIAM Jour. Numerical Analysis*, 42:1914–1931, 2005.

[3] D. N. Arnold, F. Brezzzi, and M. Fortin. A stable finite element for the Stokes equation. *Calcolo*, 21:337–344, 1984.

[4] G. S. Beavers and D. D. Joseph. Boundary conditions at a natural permable wall. *Jour. of Fluid Mechanics*, 30:197–207, 1967.

[5] D. Braess. *Finite Elements - Fast Solvers and Applications in Solid Mechanics.* Cambridge University Press, 2nd edition, 2001.

[6] S. Brenner. Korn's inequalities for picewise H^1 vector fields. *Mathematics of Computation*, 73:1067–1087, 2003.

[7] S. Brenner. Poincaré–Friedrichs inequalities for piecewise H^1 functions. *SIAM Jour. Numerical Analysis*, 41:306–324, 2003.

[8] F. Brezzi. On the existence, uniqueness and approximation of saddle-point problems arising from Lagrangian multipliers. *RAIRO Numerical Analysis*, 8:129–151, 1974.

[9] F. Brezzi and M.Fortin. *Mixed and Hybrid Finite Element Methods.* Springer, 1991.

[10] P. Clement. Approximation by finite element functions using local regularizations. *RAIRO Numerical Analysis*, 9:77–84, 1975.

[11] M. Fortin. Old and new finite elements for incompressible flows. *Int. Jour. Numerical Methods for Fluids*, 1:347–364, 1981.

[12] D. K. Gartling, C. E. Hickox, and R. C. Givler. Simulation of coupled viscous and porous flow problems. *Comp. Fluid Dynamics*, 7:23–48, 1996.

[13] G. Gatica, S. Meddahi, and R. Oyarzúa. A conforming mixed finite element method for the coupling of fluid flow with porous media flow. *Preprint 06-01, Departamento de Ingeniería Mathemática, Universidad de Concepción*, 2006.

[14] V. Girault and P.-A. Raviart. *Finite Element Methods for Navier Stokes Equations.* Springer, 1986.

[15] W. Layton, F. Schieweck, and I. Yotov. Coupling fluid flow with porous media flow. *SIAM Jour. Numerical Analysis*, 40:2195–2218, 2003.

[16] E. Miglio M. Discacciati and A. Quarteroni. Mathematical and numerical models for coupling surface and groundwater flows. *Applied Numerical Mathematics*, 43:57–74, 2002.

[17] K.-A. Mardal, X.-C. Tai, and R. Winther. A robust finite element method for the Darcy-Stokes flow. *SIAM Jour. Numerical Analysis*, 40:1605–1631, 2002.

[18] K.-A. Mardal and R. Winther. An observation on Korn's inequality for nonconforming finite element methods. *Mathematics of Computation*, 75(253):1–6, 2006.

[19] B. Rivière. Analysis of a discontinuous finite element method for the coupled Stokes and Darcy problem. *Jour. Scientific Computing*, 22:479–500, 2005.

[20] B. Rivière and I. Yotov. Locally conservative coupling of Stokes and Darcy flows. *SIAM Jour. Numerical Analysis*, 42:1959–1977, 2005.

[21] P. G. Saffmann. On the boundary conditions at the interface of a porous medium. *Studies in Applied Mathematics*, 1:93–101, 1973.

[22] A. G. Salinger, R. Aris, and J. J. Derby. Finite element formulations for large-scale, coupled flows in adjacent porous and open fluid domains. *Int. Jour. for Numerical Methods in Fluids*, 18:1185–1209, 1994.

[23] X.-C. Tai and R. Winther. A discrete de Rahm complex with enhanced smoothness. *Calcolo*, 43:287–306, 2006.

Centre of Mathematics for Applications University of Oslo, P.O. Box 1053, Blindern, 0316 Oslo, Norway

E-mail address: trygvekk@student.matnat.uio.no

Department of Scientific Computing, Simula Research Laboratory, University of Oslo, P.O.Box 134, 1325 Lysaker, Norway

E-mail address: kent-and@simula.no

Centre of Mathematics for Applications University of Oslo, P.O. Box 1053, Blindern, 0316 Oslo, Norway

E-mail address: ragnar.winther@cma.uio.no